CrossMark

ORIGINAL PAPER

Catalytic nanocrystalline coordination polymers as an efficient peroxidase mimic for labeling and optical immunoassays

Veronika Čunderlová[1] · Antonín Hlaváček[1] · Veronika Horňáková[1] ·
Miroslav Peterek[1] · Daniel Němeček[1] · Aleš Hampl[2] · Luděk Eyer[3] · Petr Skládal[1]

Abstract We report that nanocrystalline Prussian blue of the type $Fe_4[Fe(CN)_6]_3$ is a powerful peroxidase mimic for use in labeling of biomolecules. The cubic nanocrystals typically have a diameter of 15 nm and are capable of catalyzing the oxidation of colorless 3,3′,5,5′-tetramethylbenzidine in the presence of H_2O_2 to form an intensively colored product with an absorption maximum at 662 nm. The determined pseudo turnover number is ~20,000 s^{-1} which is the highest value reported for nanoparticles of a size comparable to common proteins. We also present a method for the biotinylation of the surface of these nanocrystals, and show their use in competitive bioaffinity based assays of biotin and human serum albumin. The limits of detection are 0.35 and 0.27 μg mL^{-1}, respectively. The results prove the applicability of coordination polymers for signal amplification and also their compatibility with the format of enzyme linked immunosorbent assays.

Keywords Enzyme mimic · Immunoassay · Nanoparticle · Prussian blue · Biotinylation · Transmission electron microscopy

✉ Antonín Hlaváček
  an.hlavacek@seznam.cz

[1] CEITEC - Central European Institute of Technology, Group Nanobiotechnology, Masaryk University, Kamenice 5/A35, 625 00 Brno, Czech Republic

[2] Faculty of Medicine, Department of Histology and Embryology, Masaryk University, 625 00 Brno, Czech Republic

[3] Department of Virology, Veterinary Research Institute, 62100 Brno, Czech Republic

Introduction

Enzymes are widely used in bioanalytical assays for amplification of the generated signal [1]. The principle of amplification is the catalytic conversion of substrate molecules to the easily detectable product [1]. For instance, the conversion of colorless substrate to a colorful or fluorescent product is utilized in enzyme linked immunosorbent assays (ELISAs) [1]. Peroxidases, like horseradish peroxidase, belong to the most often used enzymatic labels for immunochemical detection. More catalytically active labels with higher signal amplification generally improve the performance of the assay [2, 3]. Methods for the detection of isolated molecules (digital ELISA) further stress the importance for high signal amplification [4].

The preparation and purification of enzymes for biomolecule labeling is generally time-consuming, expensive and demanding for resources [5], which are factors limiting the sustainability of their production. Contrary, catalytic nanoparticles can be prepared at mild conditions with good efficiency, utilizing benign precursors and operating in water based dispersant [6]. The applicability of catalytic nanoparticles for practical use is also facilitated by the stability of inorganic nanomaterials [7].

Among other candidates [8], nanoparticles with high peroxidase-like activity were extensively studied for their applicability in immunochemical assays. The first discovered nanoparticles with peroxidase-like activity were composed of Fe_3O_4 [7, 9, 10]. Later on, the peroxidase-like activity of CuO [11], CeO_2 [12], MnO_2 [13], Co_3O_4 [14], bimetallic [15, 16], mesoporous silica nanoparticles modified by catalytic metal complexes [2], graphene oxide nanoplates [17] and hemin-block copolymer micelles [18] have been reported.

The class of solids defined as coordination polymers [19] is recently one of the most exciting fields in solid state chemistry. Despite the increasing number of reports describing their catalytic properties [19], the use of coordination polymers in a pure form as an enzyme mimics for biomolecule labeling was not reported. The reason may be the lack of methods for surface modification. Prussian blue [20] – one of the most prominent member of this class – was utilized in this study as a label for immunoassay.

Prussian blue, with a chemical formula $Fe_4[Fe(CN)_6]_3$ [20], has been widely used for the construction of electrochemical biosensors as an electron transfer mediator [21]. The surface of Prussian blue nanoparticles (PBNPs) contains the Fe^{3+}/Fe^{2+} redox couple, which is also responsible for the catalytic properties of peroxidases as well as Fe_3O_4 nanoparticles. Despite of this similarity, the peroxidase like activity of PBNPs has been described just recently [22]. Previously, peroxidase mimic γ-Fe_2O_3 nanoparticles coated with the layer of Prussian blue were studied [23]. The rate of TMB oxidation in the presence of H_2O_2 was increased when Prussian blue was introduced on the surface of γ-Fe_2O_3 nanoparticle. Electrostatic interactions also allowed for protein modification and bioaffinity detection.

In this contribution, PBNPs were used as a catalytic label for the bioaffinity detection of biotin and immunoassay of human serum albumin. The kinetics of catalytic conversion of the colorless substrate 3,3′,5,5′-tetramethylbenzidine to the blue-colored product is described. A method for the preparation of biotinylated PBNPs (biotin-PBNPs) was adapted from our previous work [24]. Transmission electron microscopy (TEM), dynamic light scattering, atomic force microscopy (AFM), gel electrophoresis and UV/VIS spectroscopy were used for nanomaterial characterization.

Experimental

Chemicals and materials

Tween 20, 2-amino-2-hydroxymethylpropane-1,3-diol (Tris), dimethyl sulfoxide, avidin, (+)-biotin N-hydroxysuccinimide ester, bovine serum albumin, human serum albumin, $NaBH_4$, $FeCl_3 \cdot 6H_2O$, poly-L-lysine hydrobromide (30,000–70,000 g mol^{-1}), bovine γ-globulin and 3,3′,5,5′-tetramethylbenzidine (TMB) were from Sigma (www.sigmaaldrich.com). $K_4[Fe(CN)_6]$ $\cdot 3H_2O$ was from Lachema. Poly(vinyl alcohol) (6000 g mol^{-1}) was from Polysciences (www.polysciences.com). The anti-human serum albumin mouse monoclonal antibody (IgG1 clone AL-01) was provided by Exbio (www.exbio.cz). LE Agarose was from Lonza (www.lonza.com). Milli-Q water was used through the work.

Nanoparticle synthesis

The volume of 20 mL of the aqueous 1.0 mmol L^{-1} $FeCl_3$ and 0.5 mmol L^{-1} citric acid was heated to 55 °C and mixed with 20 mL of 1.0 mmol L^{-1} $K_4[Fe(CN)_6]$ and 0.5 mmol L^{-1} citric acid under vigorous stirring. The resulting mixture was stirred for 10 min and then cooled down to room temperature [6].

Preparation of denatured bovine serum albumin

Bovine serum albumin (10 mg) and $NaBH_4$ (0.7 mg) were dissolved in 3.1 mL of water and shaken for 60 min at laboratory temperature. The mixture was subsequently heated to 80 °C for approximately 30 min to decompose the excessive $NaBH_4$. Thus prepared denatured bovine serum albumin (1.5 mL) was mixed with phosphate buffer (0.15 mL, 0.5 mol L^{-1}, pH 8.0) and 38 μL of (+)-biotin N-hydroxysuccinimide ester (20 mg mL^{-1}, dissolved in dimethyl sulfoxide). The solution of biotinylated denatured bovine serum albumin was obtained after 60 min at laboratory temperature.

Synthesis of biotinylated Prussian blue nanoparticles

The volume of 62.5 μL of the freshly prepared biotinylated albumin was dissolved in 1 mL of the assay buffer (Tris 50 mmol L^{-1}, NaCl 150 mmol L^{-1}, 0.02 % Tween 20, 0.05 % γ-globulin, 0.5 % bovine serum albumin and 0.2 % poly(vinyl alcohol) (w/v), pH 7.75). The PBNPs and the solution of biotinylated albumin were mixed in the volume ratio 1:1 and heated to 70 °C for 5 min. Biotin-PBNPs were purified by size exclusion chromatography on Sephadex G25 from GE Healthcare (www.gehealthcare.com) and assay buffer was used as a mobile phase.

Measurement of catalytic activity

The catalytic activities of PBNPs and their bioconjugates were measured at laboratory temperature in 96 well microtiter plate using the Synergy 2 reader from BioTek (www.biotek.com). Microtiter plate wells were loaded with 10 μL of dimethyl sulfoxide solution of TMB, 20 μL of water diluted H_2O_2 and 170 μL of nanomaterial dispersion in acetate buffer (200 mmol L^{-1} pH 3.5); TMB oxidation was not observed before the addition of buffer. The final concentration of PBNPs and biotin-PBNPs were 6.7×10^{-12} and 6.7×10^{-11} mol L^{-1}, respectively. The slope of the time dependence of absorbance of yellow and blue products with absorption maxima at 450 and 652 nm ($\Delta A_{450}/\Delta t$ and $\Delta A_{652}/\Delta t$), respectively, were utilized for the estimation of H_2O_2 reduction rate (v_{H2O2}). The rate of oxidation of TMB to the yellow product (v_{TMB450}) after the addition of sulfuric acid was more typically measured in previous studies.

Herein reported v_{H2O2} is equivalent to v_{TMB450} (Eq. 1). Extinction coefficients $\varepsilon_{450} = 59{,}000$ L mol^{-1} cm^{-1} and $\varepsilon_{652} = 39{,}000$ L mol^{-1} cm^{-1} and the length of optical path $l = 0.579$ cm were utilized for computation [25].

$$v_{H_2O_2} = v_{TMB450} = \left(\frac{\Delta A_{652}}{\varepsilon_{652} \times l} + \frac{\Delta A_{450}}{\varepsilon_{450} \times l} \right) \times \frac{1}{\Delta t} \qquad (1)$$

In parallel, the reaction rate without the presence of catalytic nanomaterial was measured and subtracted from reaction rate of the catalyzed reaction.

Detection of biotin

The Immobilizer Streptavidin F96 Clear microtiter plates from Nunc (www.nuncbrand.com) were used for the detection of biotin with catalytic signal amplification. Firstly, the streptavidin coated wells were loaded with assay buffer (250 µL per well) and shaken at 300 rpm for 60 min at laboratory temperature. Subsequently, the assay buffer was replaced by the mixture of free biotin (10 µL in dimethyl sulfoxide) and biotin-PBNPs in the assay buffer (90 µL, 3.3 nmol L^{-1}). The set of biotin samples of known concentrations was used for the construction of calibration curve (1000, 10, 0.1, 10^{-3}, 10^{-5}, 10^{-7}, 10^{-9} and 0 µg mL^{-1} of biotin in dimethyl sulfoxide). Microtiter plate was shaken for 60 min at laboratory temperature. After four times washing by washing buffer (phosphate 50 mmol L^{-1} pH 7.4 supplemented with 0.05 % Tween-20), color was developed by the addition of freshly prepared substrate solution (TMB 500 µmol L^{-1} and H$_2$O$_2$ 125 mmol L^{-1} in sodium acetate 0.2 mol L^{-1} pH 3.5, 100 µL per well).

Detection of human serum albumin

Competitive assay utilizing biotin-PBNPs was developed. MaxiSorp 96 well microtiter plates from Nunc (www.nuncbrand.com) were coated with human serum albumin (150 µL per well, 0.1 mg mL^{-1} in 50 mmol L^{-1} phosphate buffer pH 7.4, incubated for 120 min at laboratory temperature). Afterwards, each plate was 4× washed with washing buffer. The mixtures of biotinylated anti-human serum albumin antibody (1 µg mL^{-1}) and human serum albumin standards in 150 mmol L^{-1} NaCl and 50 mmol L^{-1} phosphate buffer pH 7.4 were combined 1:1 in test tubes and incubated for 15 min at laboratory temperature. Next, 80 µL of the resulting solution were added to the microtiter plate wells, incubated for 40 min at laboratory temperature and 4× washed. Wells were filled with 80 µL of avidin solution (40 µg mL^{-1} in 50 mmol L^{-1} phosphate buffer pH 7.4), incubated for 25 min and 4× washed. Biotin-PBNPs were added (80 µL, 3.3 nmol L^{-1}), incubated for 60 min and 4× washed.

Finally, the color was developed by the addition of freshly prepared substrate solution (TMB 500 µmol L^{-1} and H$_2$O$_2$ 125 mmol L^{-1} in sodium acetate 0.2 mol L^{-1} pH 3.5, 100 µL per well).

Results and discussion

Prussian blue nanoparticles

One step coprecipitation method was used for the preparation of PBNPs [6]. The cubic shape of PBNPs was revealed with transmission electron microscopy (Fig. 1). The length of the edge of PBNP cubes was 15.3 ± 3.4 nm and the average surface area of nanocrystals was 1400 nm^2. Assuming the distance of Fe^{2+} and Fe^{3+} ions of 0.51 nm in the nanocrystal [20], then average number of Fe^{2+} and Fe^{3+} ions in a single PBNP was ~30,000 and the concentration [27] of the prepared PBNPs was 33 nmol L^{-1}.

Catalytic properties

Catalytic oxidation of TMB in the presence of H$_2$O$_2$ with Prussian blue coated γ-Fe$_2$O$_3$ NPs was previously reported [23]. However, pure PBNPs with regular shape were used in this study allowing better catalytic characterization. PBNPs mimic the peroxidase activity of horseradish peroxidase converting colorless TMB to colored products (Fig. S1, S2 in the Electronic Supplementary Material – ESM). The first oxidation product is the blue charge-transfer complex of the diamine and the diimine with absorption maxima at 652 nm.
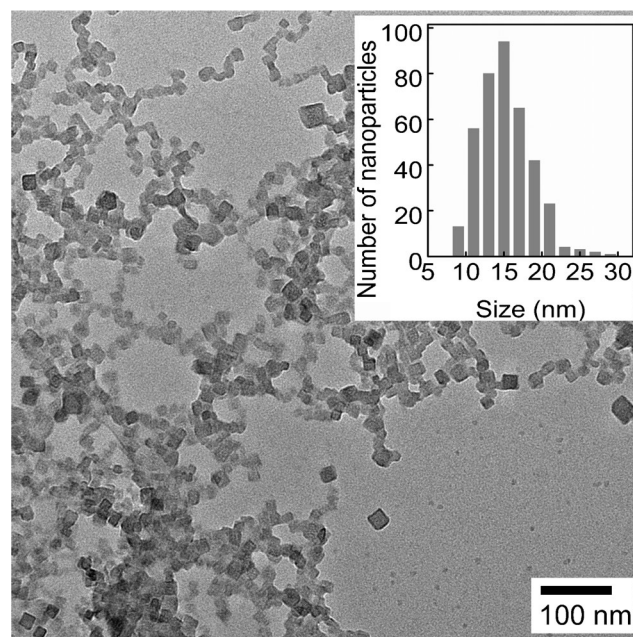

Fig. 1 TEM image of PBNPs with size distribution plotted as an inset

The blue product is further oxidized to yellow 3,3′,5,5′-tetramethylbenzidine diimine with absorption maxima at 450 nm [25]. We applied the model of Michaelis-Menten to characterize kinetic parameters of the catalyzed reaction (Fig. 2, Eq. 2):

$$v_{H_2O_2} = \frac{S \times V_L}{S + K_M} \qquad (2)$$

Where v_{H2O2} is the initial rate of H_2O_2 reduction, S is substrate concentration, K_M is Michaelis constant, V_L is maximum value of v_{H2O2} at saturating concentration of substrate. Kinetic parameters for both substrates were estimated independently keeping high concentration of the complementary substrate (H_2O_2 1000 mmol L^{-1}, TMB 500 μmol L^{-1} was close to the solubility of TMB, which is ~800 μmol L^{-1}). The estimated values of K_M for TMB was 0.76 ± 0.21 mmol L^{-1}, which is comparable with values estimated for previously published catalytic nanoparticles and similar to K_M of horseradish peroxidase. The value of K_M for H_2O_2 was 840 ± 160 mmol L^{-1}. This value is comparable with K_M of Co_3O_4, Fe_3O_4 and Prussian blue coated γ-Fe_2O_3 nanoparticles and is substantially higher than K_M of horseradish peroxidase and mesoporous silica nanoparticles modified by catalytic metal complexes (Table 1).

Based on the V_L values, PBNPs possess the highest turn-over number (k_{cat}) between nanoparticles with size smaller than 20 nm, e.i., the size comparable with the size of proteins.
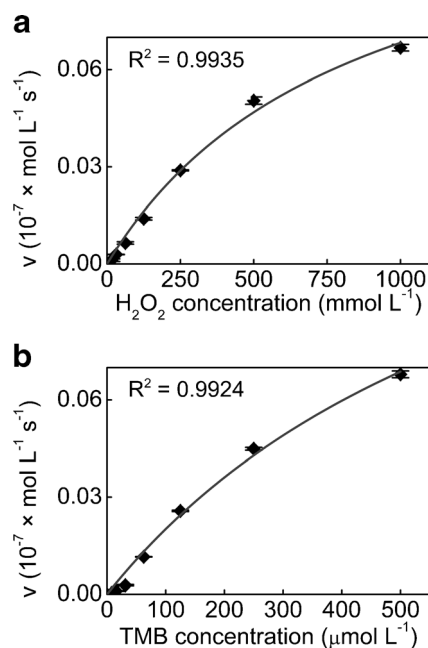
a
$R^2 = 0.9935$

y-axis: v ($10^{-7} \times$ mol L^{-1} s^{-1})
x-axis: H_2O_2 concentration (mmol L^{-1})

b
$R^2 = 0.9924$

y-axis: v ($10^{-7} \times$ mol L^{-1} s^{-1})
x-axis: TMB concentration (μmol L^{-1})

Fig. 2 Kinetic parameters of Prussian blue nanoparticles. The estimation of K_M and V_M with fixed concentration of **a** 3,3′,5,5′-tetramethylbenzidine (TMB, 500 μmol L^{-1}) and **b** H_2O_2 (1000 mmol L^{-1}). The concentration of Prussian blue nanoparticles was 6.7×10^{-12} mol L^{-1}

The value of k_{cat} of PBNPs is approximately $30\times$ higher than k_{cat} of horseradish peroxidase. To compare between differently sized nanoparticles of different materials, the values of k_{cat} were divided with the surface area of particular nanoparticle (A) and reported as a ratio k_{cat}/A (Table 1). The value of k_{cat}/A of Prussian blue coated γ-Fe_2O_3 was slightly lower than k_{cat}/A of pure PBNPs, which is probably the result of incomplete surface modification of γ-Fe_2O_3 nanoparticles. Assuming only outer surface of nanoparticle for computation then the highest value of k_{cat}/A was obtained for 40 nm mesoporous silica nanoparticles modified by catalytic metal complexes [2]. However, the actual catalytic surface consisting of mesoscopic pores is substantially higher. Therefore, the value of k_{cat}/A should be considered a rather comparable with PBNPs.

Biotinylated Prussian blue nanoparticles

The synthesis of PBNPs was carried out with the expected result in the presence of citric acid as a stabilizing ligand. Although citric acid contains –COOH groups, its applicability for the synthesis of stable bioconjugates is limited. The reason is low stability of monodentate ligands on the surface of NPs. A common solution for this problem is the introduction of multidentate polymeric ligands [24]. Multiple interactions of polymeric ligands allows for stable surface modification and subsequent covalent attachment of biomolecules, e.g., biotin and others. According to this principle, reductively denatured bovine serum albumin was utilized as a polymeric ligand possessing a number of functional groups coordinating the surface of PBNPs (residues of lysine, histidine, cysteine and glutaric and aspartic acids). Folded structure of native bovine serum albumin was relaxed in the presence of $NaBH_4$ at elevated temperature. Disulfide bridges in its structure were broken and readily attached the surface of PBNPs. Similarly, biotinylated albumin was used resulting in biotin-PBNP (Fig. S3, ESM).

The biotinylation of PBNPs was confirmed with agarose gel electrophoresis as a shift of electrophoretic mobility (Fig. 3c and S4, ESM) [26]. Dynamic light scattering also revealed increased hydrodynamic diameter of biotin-PBNPs (Fig. S5, ESM). Considering the surface area of single PBNP and single molecule of albumin, the optimal molar ratio is ~73 (Fig. S6, ESM). The experimentally found optimal concentration of PBNPs and biotinylated albumin in bioconjugation mixture was ~16 and 2200 nmol L^{-1}, respectively (molar ratio ~140). The microscopic structure of this bioconjugate was investigated with TEM and AFM (Fig. 3a, b and S7, ESM). Both methods revealed partial aggregation of biotin-PBNPs. Bioconjugate size ranges from single PBNPs to aggregates containing hundreds of PBNPs with diameter of ~500 nm. This observation was in agreement with agarose gel electrophoresis (Fig. 3c) and refers for self limiting size of

Table 1 Catalytic properties of horseradish peroxidase and horseradish peroxidase mimic nanoparticles. All reported values were measured at laboratory temperature. $[NP]$ is the particle concentration, K_M is the Michaelis constant, and k_{cat} is turnover number; $k_{cat} = V_L/[NP]$ where V_L is limiting reaction rate. The ratio of k_{cat}/A is k_{cat} per unit area of catalytic surface A

Type	Size (nm) Shape	Substrate	$[NP]$ [mol L^{-1}]	K_M [mmol L^{-1}]	k_{cat} [s^{-1}]	k_{cat}/A [s^{-1} nm^{-2}]
PBNP *This work*	15.3	TMB	6.7×10^{-12}	0.76 ± 0.21	26000 ± 4900	19 ± 4
	Cube	H$_2$O$_2$		840 ± 160	$19,000 \pm 2000$	13 ± 2
Biotin-PBNP *This work*	-	TMB	6.7×10^{-11}	-	-	-
	-	H$_2$O$_2$		1130 ± 230	1610 ± 210	-
Prussian blue coated γ-Fe$_2$O$_3$ [23]	10.5	TMB	3.09×10^{-10}	0.307	3430	9.9
	Sphere	H$_2$O$_2$		323.6	3,790	10.9
Co$_3$O$_4$ [14]	7.2	TMB	2.53×10^{-9}	0.103 ± 0.015	101 ± 3.2	0.62 ± 0.02
	Sphere	H$_2$O$_2$		174 ± 57	74.7 ± 8.7	0.46 ± 0.05
Fe$_3$O$_4$ [14]	8.1	TMB	7.92×10^{-9}	0.233 ± 0.006	22.2 ± 0.13	0.108 ± 0.006
	Sphere	H$_2$O$_2$		480 ± 117	34.7 ± 4.6	0.17 ± 0.02
MnO$_2$ [13]	~5	TMB	3.01×10^{-8}	0.04	192	2.4
	Sphere	H$_2$O$_2$		-	-	-
Au@Pt [15]	67 × 18.3	TMB	1.25×10^{-11}	0.027	14,480	3.3
	Rod	H$_2$O$_2$		-	-	-
Fe-MSN [2]	40	TMB	1.25×10^{-13}	0.122	2.65×10^6	527[a]
	Sphere	H$_2$O$_2$		6.67	2.60×10^6	517[a]
Horseradish peroxidase [28]	-	TMB	1×10^{-9}	0.147	790	-
	-	H$_2$O$_2$		0.146	782	-

[a] Outer surface area of mesoporous silica nanoparticles modified by catalytic metal complexes (Fe-MSN) was used to estimate k_{cat}/A

biotin-PBNP aggregates [29]. The aggregates moved as a single electrophoretic zone in 0.8 % electrophoretic agarose gel. Contrary, 2.0 % agarose with smaller pores revealed the presence of bigger aggregates possessing nearly zero electrophoretic mobility. Higher concentration of biotinylated albumin (molar ratio ~ 1400) also resulted in bioconjugates with a similar electrophoretic pattern (Fig. S4, ESM). However, the possible presence of free biotinylated albumin may compromise bioaffinity assays. When lower concentration of biotinylated albumin was used (molar ratio ~ 14), the resulting biotin-PBNPs were more aggregated, which is probably the consequence of multiple binding sides of albumin resulting in nanomaterial crosslinking (Fig. S4, ESM).

Biotin-PBNPs retained catalytic activity towards TMB and H$_2$O$_2$ (Fig. S8). Interestingly, the dependence of v_{H2O2} on the concentration of TMB was not well fitted with the model of Michaelis-Menten. The linear dependence of v_{H2O2} suggests that v_{H2O2} is limited by the rate of diffusion of TMB through the biotinylated surface. Diffusion limitation was not observed for the dependence on the concentration of much smaller H$_2$O$_2$. The value of K_M was 1130 ± 230 mmol L^{-1}, which is slightly higher than K_M of bare PBNPs. The value of k_{cat} was reduced approximately twelve times to 1610 ± 210 s^{-1}. This decrease of catalytic activity is probably caused by diffusion barrier on the catalytic surface and partial aggregation.

Nevertheless, k_{cat} of biotin-PBNPs was still ~2× higher than k_{cat} of horseradish peroxidase.

Bioaffinity detection

Biotin-PBNPs were purified by gel filtration on Sephadex G25. The elution with assay buffer removed impurities with small molecular mass including free biotin, which would otherwise interfere in bioaffinity assays. Biotin-PBNPs provided excellent competition with free biotin for streptavidin on the microtiter plate (Fig. 4a, b and S9, ESM). Calibration curve for the detection of biotin was constructed for biotin concentrations from zero to 1000 μg mL^{-1}; results were fitted to a four-parameter logistic function (ESM) and LOD of 0.35 μg mL^{-1} was estimated (Fig. 4b). Specificity of the biotin-PBNPs interaction with streptavidin was further tested with PBNPs coated with biotin-free albumin. When this blank was utilized, neither adsorption nor competition was observed (Fig. S9, ESM).

Biotin-(strept)avidin interaction provides an important alternative to increase the sensitivity of immunoassays [30]. Herein, biotin-avidin amplification system was adapted for the competitive immunochemical detection of human serum albumin (Fig. 4c, d). At first, microtiter plate was coated with human serum albumin. After washing, the mixtures of standards with known concentration of human serum albumin and
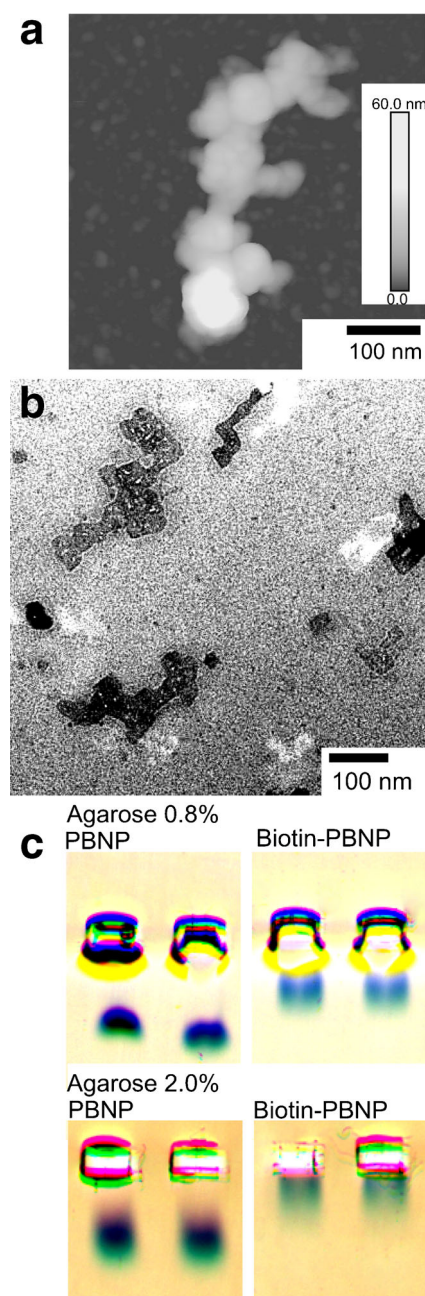
Fig. 3 Biotinylated Prussian blue. **a** AFM and **b** TEM images revealed partial aggregation of biotinylated Prussian blue. **c** Agarose gel electrophoresis of Prussian blue (PBNP) and biotinylated Prussian blue (biotin-PBNP) using two gel concentrations
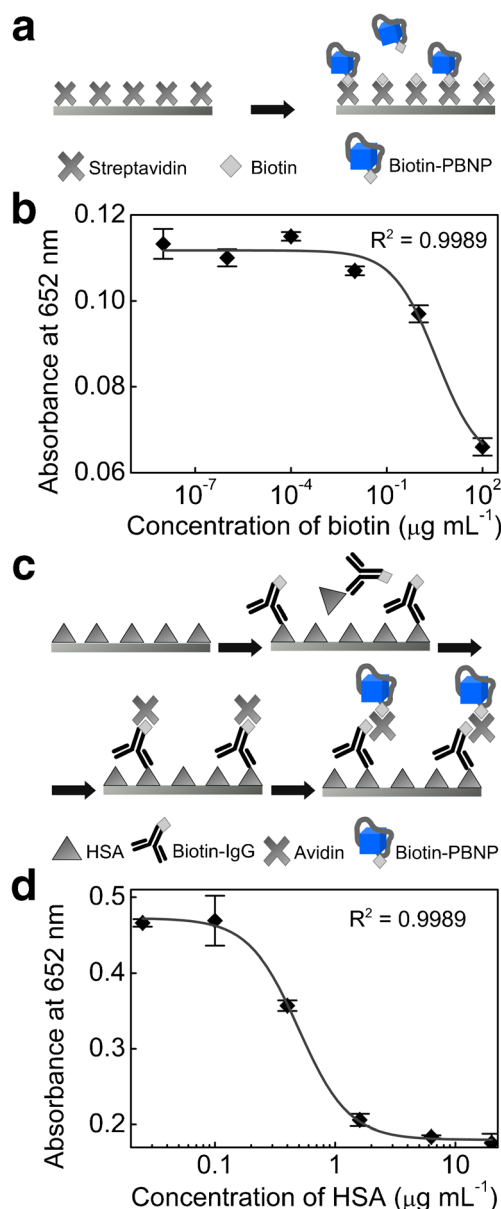

Fig. 4 Bioaffinity assays. **a** The scheme of competitive detection of biotin. Microtiter plate coated with streptavidin was incubated with the mixture of biotinylated PBNPs (biotin-PBNPs) and different concentrations of free biotin. **b** Absorbance increased with decreasing concentration of free biotin. **c** The scheme of competitive detection of human serum albumin (HSA). Microtiter plate coated with human serum albumin was incubated with biotinylated anti-human serum albumin IgG (biotin-IgG). Specifically adsorbed antibody was detected with avidin-biotin amplification system. **d** Absorbance increased with decreasing concentration of human serum albumin

biotinylated anti-human serum albumin IgG were loaded. Biotinylated antibody was detected with the sequential attachment of avidin and biotin-PBNPs. The incubation of microtiter plates with TMB/H_2O_2 substrate solution for 30 min was sufficient for the construction of calibration curve (Fig. 4d). The acquired data were fitted with logistic function (ESM). The LOD for human serum albumin was 0.27 µg mL^{-1} and the total time of analysis was 170 min, which is not that much critical due to the parallel processing of samples in

microplates. The achieved LOD is just 3× higher than chemi-luminescent method (0.089 µg mL^{-1}) [31] and approximately ten times lower than immunoturbidimetry and other methods, which are standard for the analysis of urine samples [24, 32]. The concentration range typical for microalbuminuria is from 20 to 200 µg mL^{-1} in 24-h urine specimens [33], which suggests for practical applicability.

Conclusion

The value of k_{cat}/A obtained for Prussian blue nanoparticles substantially exceeds k_{cat}/A of Fe_3O_4, Co_3O_4, MnO_2 and Au@Pt nanoparticles and was also higher than k_{cat}/A of Prussian blue coated γ-Fe_2O_3 nanoparticles. The value of k_{cat}/A for mesoporous silica nanoparticles modified by catalytic metal complexes was comparable when overall surface area was assumed. The protocol for surface biotinylation is presented. Biotinylated PBNPs were utilized for competitive bioaffinity assay of biotin with the limit of detection 0.35 µg mL^{-1}. The compatibility with ELISA technology was demonstrated in immunoassay of human serum albumin with the limit of detection 0.27 µg mL^{-1}. The simplicity of PBNPs synthesis is in contrast to the purification of enzymes from biological materials. Assuming the variety of composition, structures and tailorability of coordination polymers, further improvement of catalytic properties and bioassay performance should be expected.

References

1. Wild D (2013) The immunoassay handbook. Theory and applications of ligand binding, ELISA and related techniques. Elsevier, Oxford, Fourth Edition
2. Kumari S, Dhar BB, Panda C, Meena A, Sen Gupta S (2014) Fe-TAML encapsulated inside mesoporous silica nanoparticles as peroxidase mimic: femtomolar protein detection. ACS Appl Mater Interfaces 6:13866–13873
3. Jackson TM, Ekins RP (1986) Theoretical limitations on immunoassay sensitivity. Current practice and potential advantages of fluorescent Eu^{3+} chelates as Non-radioisotopic tracers. J Immunol Methods 87:13–20
4. Walt DR (2013) Optical methods for single molecule detection and analysis. Anal Chem 85:1258–1263
5. Lavery CB, MacInnis MC, MacDonald MJ, Williams JB, Spencer CA, Burke AA, Irwin DJG, DöCunha GB (2010) Purification of peroxidase from horseradish (Armoracia rusticana) roots. J Agric Food Chem 58:8471–8476
6. Shokouhimehr M, Soehnlen ES, Khitrin A, Basu S, Huang SD (2010) Biocompatible Prussian blue nanoparticles: preparation, stability, cytotoxicity, and potential use as an MRI contrast agent. Inorg Chem Commun 13:58–61
7. Gao L, Zhuang J, Nie L, Zhang J, Zhang Y, Gu N, Wang T, Feng J, Yang D, Perrett S, Yan X (2007) Intrinsic peroxidase-like activity of ferromagnetic nanoparticles. Nat Nanotechnol 2:577–583
8. Wei H, Wang E (2013) Nanomaterials with enzyme-like characteristics (nanozymes): next-generation artificial enzymes. Chem Soc Rev 42:6060–6093
9. Zhang Z, Zhu H, Wang X, Yang X (2011) Sensitive electrochemical sensor for hydrogen peroxide using Fe_3O_4 magnetic nanoparticles as a mimic for peroxidase. Microchim Acta 174:183–189
10. Chang Q, Deng K, Zhu L, Jiang G, Yu C, Tang H (2009) Determination of hydrogen peroxide with the aid of peroxidase-like Fe_3O_4 magnetic nanoparticles as the catalyst. Microchim Acta 165:299–305
11. Chen W, Chen J, Liu A-L, Wang L-M, Li G-W, Lin X-H (2011) Peroxidase-like activity of cupric oxide nanoparticle. ChemCatChem 3:1151–1154
12. Xu C, Qu X (2014) Cerium oxide nanoparticle: a remarkably versatile rare earth nanomaterial for biological applications. NPG Asia Mater 6 (3) art. no. e90
13. Liu X, Wang Q, Zhao H, Zhang L, Su Y, Lv Y (2012) BSA-templated MnO_2 nanoparticles as both peroxidase and oxidase mimics. Analyst 137:4552–4558
14. Dong J, Song L, Yin J-J, He W, Wu Y, Gu N, Zhang Y (2014) Co_3O_4 nanoparticles with multi-enzyme activities and their application in immunohistochemical assay. ACS Appl Mater Interfaces 6:1959–1970
15. He W, Liu Y, Yuan J, Yin J-J, Wu X, Hu X, Zhang K, Liu J, Chen C, Ji Y, Guo Y (2011) Au@Pt nanostructures as oxidase and peroxidase mimetics for use in immunoassays. Biomaterials 32:1139–1147
16. Zhang Y, Lu F, Yan Z, Wu D, Ma H, Du B, Wei Q (2015) Electrochemiluminescence immunosensing strategy based on the use of Au@ Ag nanorods as a peroxidase mimic and NH_4CoPO_4 as a supercapacitive supporter. Microchim Acta 182:1421–1429
17. Song Y, Qu K, Zhao C, Ren J, Qu X (2010) Graphene oxide: intrinsic peroxidase catalytic activity and its application to glucose detection. Adv Mater 22:2206–2210
18. Qu R, Shen L, Chai Z, Jing C, Zhang Y, An Y, Shi L (2014) Hemin-block copolymer micelle as an artificial peroxidase and its applications in chromogenic detection and biocatalysis. ACS Appl Mater Interfaces 6:19207–19216
19. Kitagawa S, Kitaura R, Noro S-I (2004) Functional porous coordination polymers. Angew Chem Int Ed 43:2334–2375
20. Herren F, Fischer P, Ludi A, Hälg W (1980) Neutron diffraction study of Prussian blue, $Fe_4[Fe(CN)_6]_3 \cdot xH_2O$. Location of water molecules and long-range magnetic order. Inorg Chem 19:956–959
21. Ricci F, Palleschi G (2005) Sensor and biosensor preparation, optimisation and applications of Prussian blue modified electrodes. Biosens Bioelectron 21:389–407
22. Zhang W, Ma D, Du J (2014) Prussian Bue nanoparticles as peroxidase mimetics for sensitive colorimetric detection of hydrogen peroxide and glucose. Talanta 120:362–367
23. Zhang X-Q, Gong S-W, Zhang Y, Yang T, Wang C-Y, Gu N (2010) Prussian blue modified iron oxide magnetic nanoparticles and their high peroxidase-like activity. J Mater Chem 20:5110–5116
24. Hlavacek A, Bouchal P, Skládal P (2012) Biotinylation of quantum dots for application in fluoroimmunoassays with biotin-avidin amplification. Microchim Acta 176:287–293
25. Josephy PD, Eling T, Mason RP (1982) The horseradish peroxidase-catalyzed oxidation of 3,5,3′,5′-tetramethylbenzidine. Free radical and charge-transfer complex intermediates. J Biol Chem 257:3669–3675
26. Hlaváček A, Sedlmeier A, Skládal P, Gorris HH (2014) Electrophoretic characterization and purification of silica-coated

photon-upconverting nanoparticles and their bioconjugates. ACS Appl Mater Interfaces 6:6930–6935

27. Shang J, Gao X (2014) Nanoparticle counting: towards accurate determination of the molar concentration. Chem Soc Rev 43: 7267–7278

28. Metelitza DI, Karasyova EI (2002) Activation of peroxidase-catalyzed oxidation of 3,3′,5,5′-tetramethylbenzidine with poly(salicylic acid 5-aminodisulfide). Biochem Mosc 67: 1048–1054

29. Xia Y, Nguyen TD, Yang M, Lee B, Santos A, Podsiadlo P, Tang Z, Glotzer SC, Kotov NA (2011) Self-assembly of self-limiting mono-disperse supraparticles from polydisperse nanoparticles. Nat Nanotechnol 6:580–587

30. Kendall C, Ionescu Matiu I, Dreesman GR (1983) Utilization of the biotin/avidin system to amplify the sensitivity of the enzyme-linked immunosorbent assay (ELISA). J Immunol Methods 56:329–339

31. Zhao L, Lin J-M, Li Z (2005) Comparison and development of two different solid phase chemiluminescence ELISA for the determination of albumin in urine. Anal Chim Acta 541:199–207

32. Kessler MA, Meinitzer A, Peter W, Wolfbeis OS (1997) Microalbuminuria and borderline-increased albumin excretion determined with a centrifugal analyzer and the albumin blue 580 fluorescence assay. Clin Chem 43:996–1002

33. Doumas BT, Peters Jr T (1997) Serum and urine albumin: a progress report on their measurement and clinical significance. Clin Chim Acta 258:3–20